Wind and Structures, *Vol. 18, No. 4 (2014) 457-471*
DOI: http://dx.doi.org/10.12989/was.2014.18.4.457

International high-frequency base balance benchmark study

John D. Holmes[*1] and Tim K.T. Tse[2a]

[1]*JDH Consulting, Mentone, Victoria 3194, Australia*
[2]*Department of Civil and Environmental Engineering, HKUST, Clearwater Bay, Hong Kong*

(Received August 13, 2012, Revised April 11, 2013, Accepted October 5, 2013)

Abstract. A summary of the main results from an international comparative study for the high-frequency base balance is given. Two buildings were specified – a 'basic' and an 'advanced' building. The latter had more complex dynamic response with coupled modes of vibration. The predicted base moments generally showed good agreement amongst the participating groups, but less good agreement was found for the roof accelerations which are dominated by the resonant response, and subject to measurement errors for the generalized force spectra, to varying mode shape correction techniques, and different methods used for combining acceleration components.

Keywords: base-balance; building; tall; vibration; wind-loading

1. Introduction

The High Frequency Base Balance (HFBB) (also known as the High-Frequency *Force* Balance (HFFB)), has been widely used as a wind-tunnel tool for determining overall wind loading and dynamic response of tall buildings to wind, for about thirty years. The basic principles have been described by Tschanz and Davenport (1983) and Boggs and Peterka (1989).

However, although the same basic principles are applied, a variety of approaches have been used to deal with, for example:

- Calculation of resonant response
- Twist (torsional) modes of vibration
- Nonlinear mode shapes
- Coupled mode shapes
- Closely-spaced frequencies
- Combined acceleration components

At a meeting held at the 12th International Conference on Wind Engineering (Cairns, Australia, July 2007), it was agreed that an International HFBB Comparison project should be initiated (Holmes *et al.* 2008). Two model tall buildings were defined, and various participating wind-tunnel laboratories manufactured their own models and carried out the tests, and

∗Corresponding author, Director, E-mail: john.holmes@jdhconsult.com
[a] Assistant Professor

http://www.techno-press.org/?journal=was&subpage=8 ISSN: 1226-6116 (Print), 1598-6225 (Online)

subsequently presented results for comparison. Groups would not be named explicitly in any reporting of the study.

The two buildings comprised:

- A 'basic' test building intended primarily for use as a benchmark for newer groups ('Building B') (Fig. 1),
- An 'advanced' building specification for more experienced groups ('Building A') (Fig. 2).

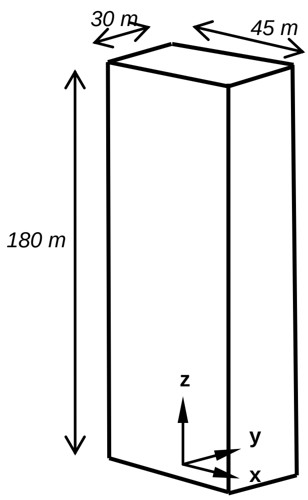

Fig. 1 'Basic' Building B for HFBB Comparison

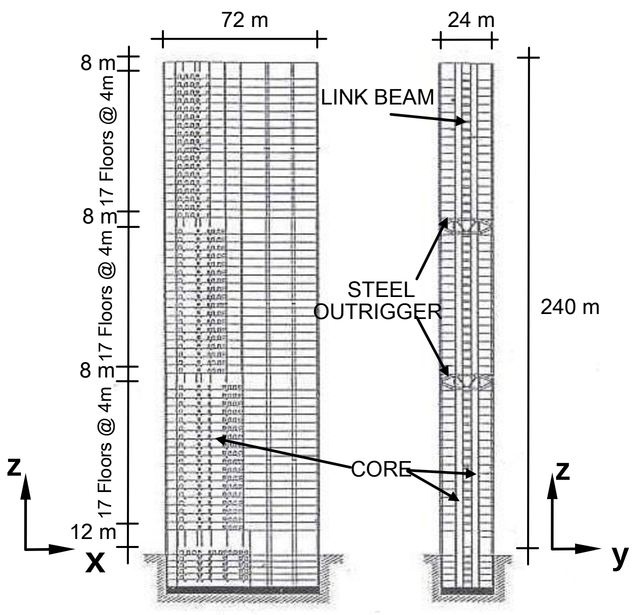

Fig. 2 'Advanced' Building A for HFBB Comparison

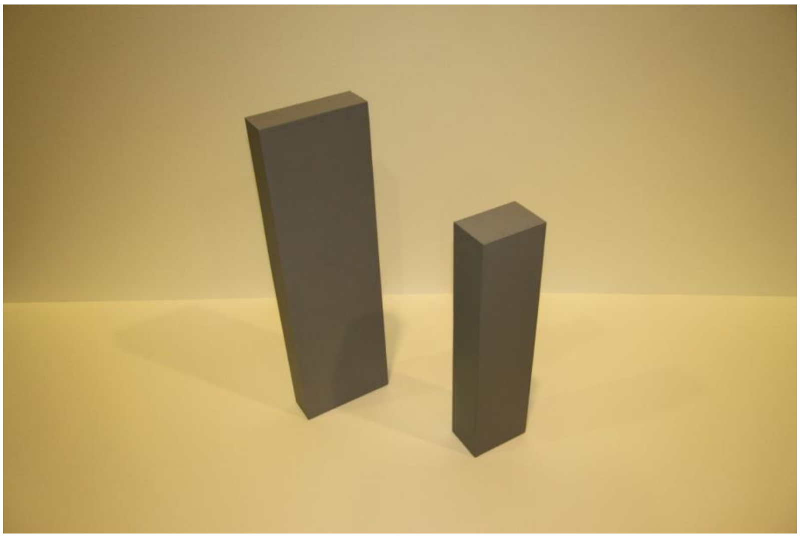

Fig. 3 The two building models used by one of the participating groups (Building A on the left; Building B on the right)

The experimental part of this study is now complete – eight groups submitted results. The eight groups include four universities and four commercial wind testing companies. Geographically the groups were from Canada (two), and one from each of United States, Australia, Korea, China, Japan and Hong Kong. The study was endorsed by the International Association for Wind Engineering (www.iawe.org) and the full specifications for the study were made available on the website of the IAWE.

The models used by one of the participating groups are shown in Fig. 3.

This paper presents some results from the analysis of the data for base moments (bending and torsional moments), and for accelerations at the top of the buildings.

Note that the integration of wind climate, particularly the variation of extreme winds and response with wind direction, are an important part of the processing of base balance data, and a source of variability between laboratories engaged in commercial testing of buildings. However, these aspects were not investigated in the comparisons described herein. They involve methods outside the base balance technique itself and should be the subject of other surveys or comparisons. In the present study, the mean wind speeds at the top of the buildings were fixed and were assumed invariant with wind direction.

It should also be noted that the validity of the base-balance technique as a method for determining the wind loads on tall buildings, including dynamic effects, has been assumed in this study and in this paper. The known limitations of the technique include an inability to accurately correct the torsional responses for mode shape, and significant approximations required in developing equivalent static load distributions with height. These limitations can be accommodated within the alternative simultaneous pressure measurement technique. That and other alternative techniques have not been addressed in this paper, which simply considers the potential variability within the known HFBB method, between different groups applying the method.

2. Comparison of basic building results

The ‘basic’ building was 180 metres in height and had cross sectional dimensions of 45 metres by 30 metres, as shown in Fig. 1. The sway frequencies were prescribed to be 0.20 and 0.23 Hertz, and the third (twist) mode has a frequency of 0.40 Hertz. All three mode shapes are assumed to vary linearly with height. The characteristics of the approaching boundary layer flow (applicable to both the basic and advanced building) are listed in Appendix A.

Seven groups submitted results for this building. One group of the total of eight did not submit results for the basic building.

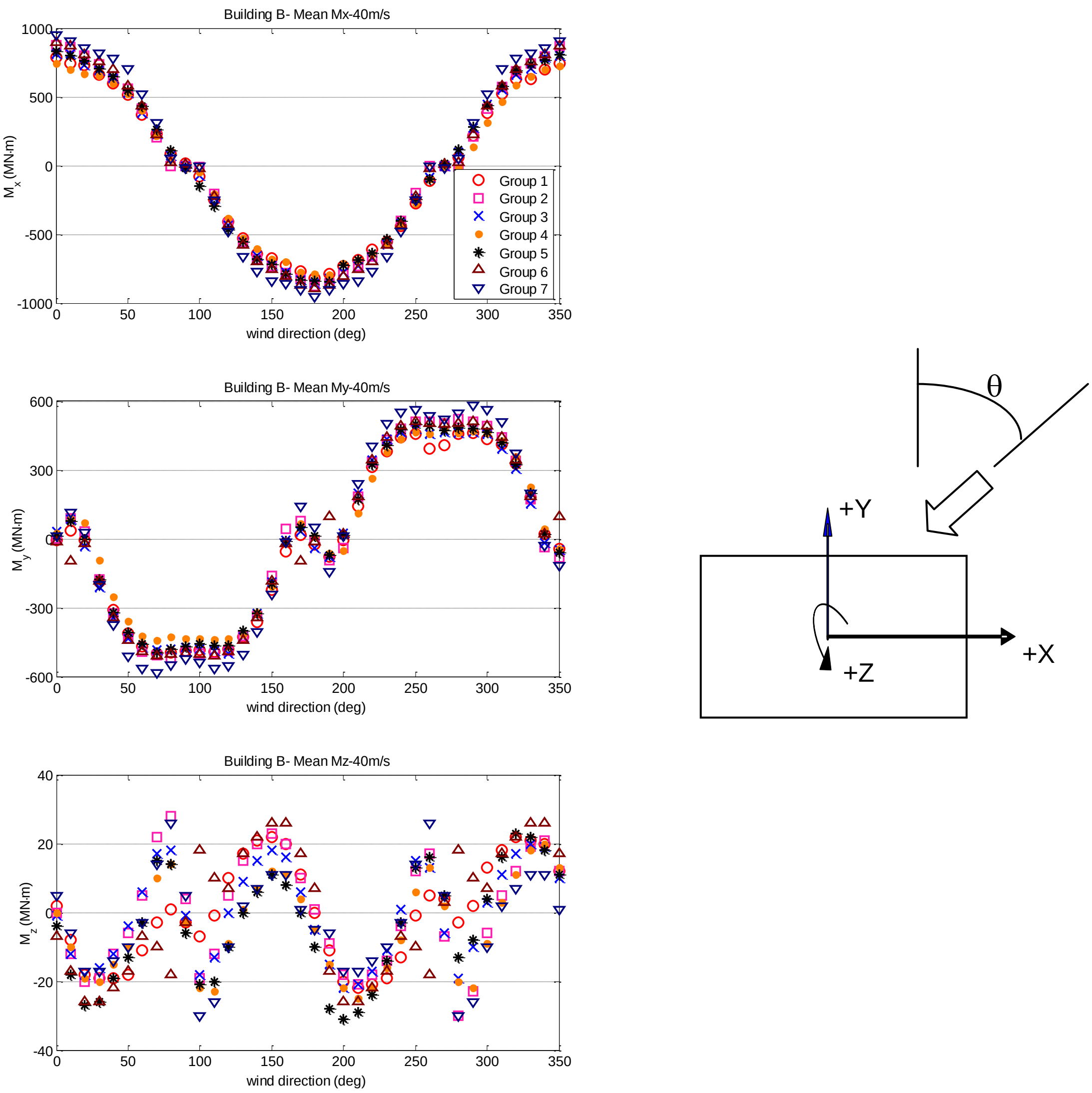

Fig. 4 Mean base moments ($\overline{U}_h$ = 40 m/s) and sign convention (Building B)

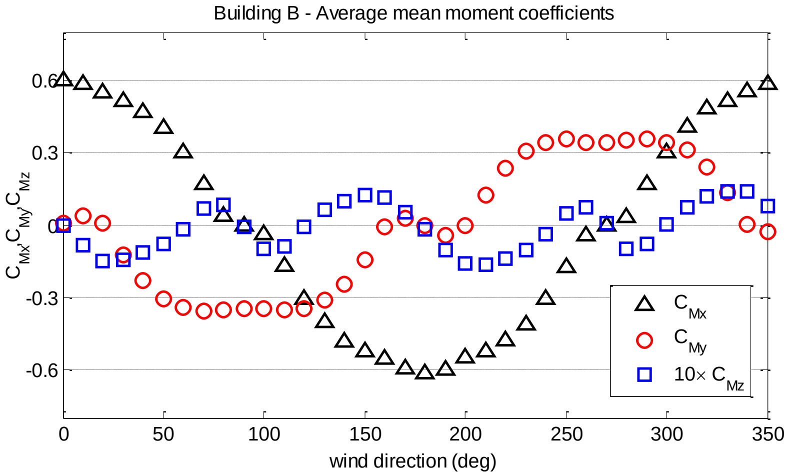

Fig. 5 Averaged mean moment coefficients for Building B

2.1 Base moment comparison - Building B

Fig. 4 shows the mean base moments for a mean wind speed at the top of the building of 40 m/s, from the seven different laboratories. The mean sway moments show good agreement, with coefficients of variation of about 8-10% for the largest values. The mean torsional moments show more scatter, although the magnitudes are considerably smaller than the sway moments. To account for varying air density used by the various groups, the results have been corrected to a sea level density of 1.20 kg/m^3. These corrections varied between 0 and 8%.

The mean base moments have been averaged over the seven sets of results, and converted to coefficients by the following

$$C_M = \frac{M}{0.5\rho\bar{U}_h{}^2 bh^2} \tag{1}$$

where $\bar{U}_h$ is the mean wind speed at the top of the building (i.e., 40 m/s in this case), b is the breadth (i.e., 45 metres), and h is the building height (i.e., 180 metres). A sea level air density of 1.2 kg/m^3 has been assumed for the calculation of coefficients.

The resulting coefficients have been plotted against wind direction, and are shown in Fig. 5. In this plot, the mean torsional moment, $\bar{C}_{Mz}$ has been multiplied by 10 for more clarity. The mean sway moment coefficients, $\bar{C}_{Mx}$ and $\bar{C}_{My}$ can be directly compared with those obtained from an earlier benchmark study for an aeroelastic model of a building with very similar dimensions – the ‘CAARC’ building, as reported by Melbourne (1980). Generally the agreement is good, although the individual measurements in the earlier study showed more scatter, perhaps reflecting less reliable experimental techniques at that time.

The predicted *maximum* base moments about the x axis for a wind speed of 40 m/s and critical damping ratio of 2.5%, are shown in Fig. 6. *Minimum* base moments about the y-axis (note the sign convention in Fig. 1) are shown for the same wind speed and damping in Fig. 7. The maximum moments about the z axis (i.e., twisting moments) are shown in Fig. 8.

The maximum base moments include fluctuating resonant components obtained by computation. These are sensitive to the measurements of spectra by the HFBB, the method of integration and the mode shape correction in the case of the torsional moment (M_z). Note that the sway moments should not require mode shape corrections for Building B, as they were specified to be linear for this building (unless the measurement height was not at ground level – this correction was left to the discretion of the group).

Probably as a result of the above complexities and sources of differences, the coefficients of variation of these results are greater than those for the mean base moments – about 15-20%, but are generally acceptable.

2.2 Comparison of accelerations – Building B

The participating groups were also asked to provide resultant accelerations at the top of the building at the geometric centre, and at a corner of the roof, for three different wind speeds. The corner accelerations incorporate the twist component of motion, as well as the sway motions. Results were provided for two damping ratios – 1% and 2.5%, although in practical terms the former value is the more relevant one for serviceability assessments

Fig. 9 shows predicted maximum corner accelerations for the building with damping of 1% of critical, and for a wind speed at the top of the building of 20 m/s. Note that two groups did not provide data for these conditions.

There is a fair amount of scatter in the predicted maximum accelerations (for any wind direction), between 7.2 and 13.3 milligs.

Acceleration calculations from a high-frequency base balance are dominated by the resonant components of the response, which are not measured but are calculated from the spectral densities of the measured base moment spectra. They are thus sensitive to measurements of the spectra at high frequencies, particularly at the high reduced frequencies associated with serviceability wind speeds. Factors such as the methods used for windowing and smoothing of the spectra and how they are corrected for model/balance resonance if necessary, as well as mode shape corrections to both sway and twist modes, and the method used to integrate for the resonant response, also play a role.

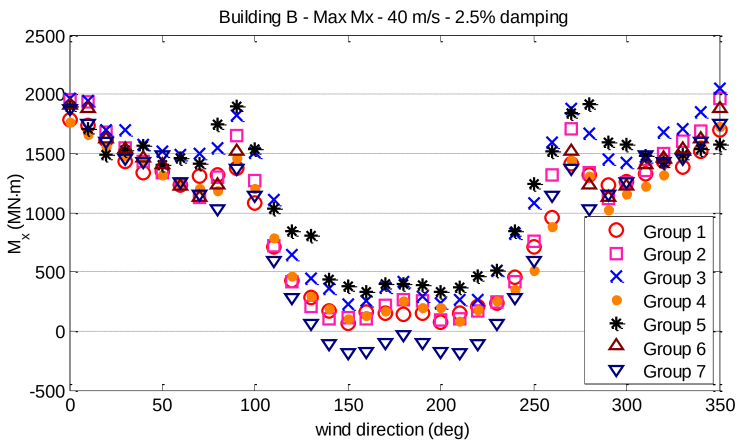

Fig. 6 Predicted maximum sway moments about the x-axis (Building B)

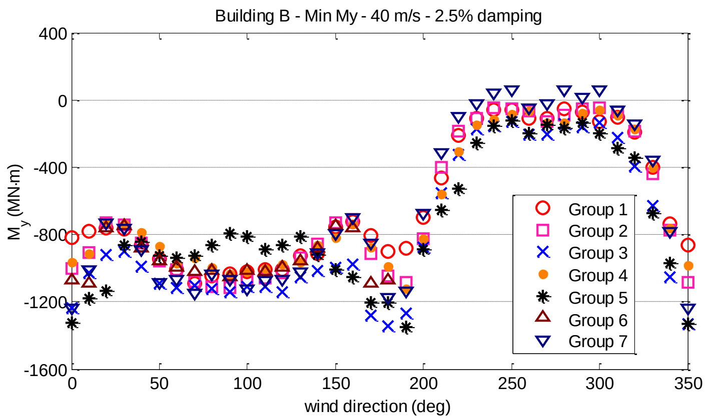

Fig. 7 Predicted minimum sway moments about the y-axis (Building B)

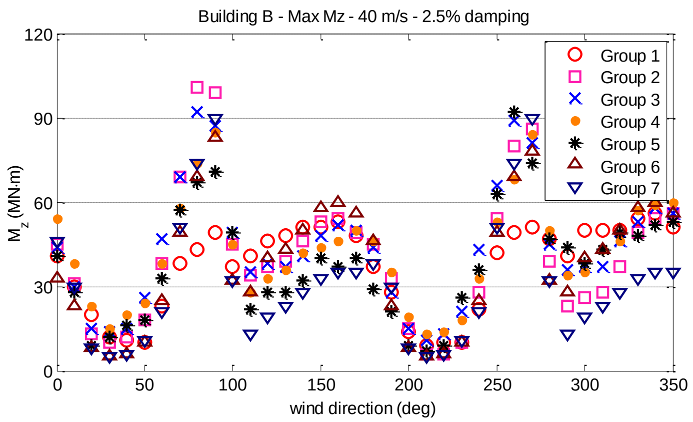

Fig. 8 Predicted maximum twist moments about the x-axis (Building B)

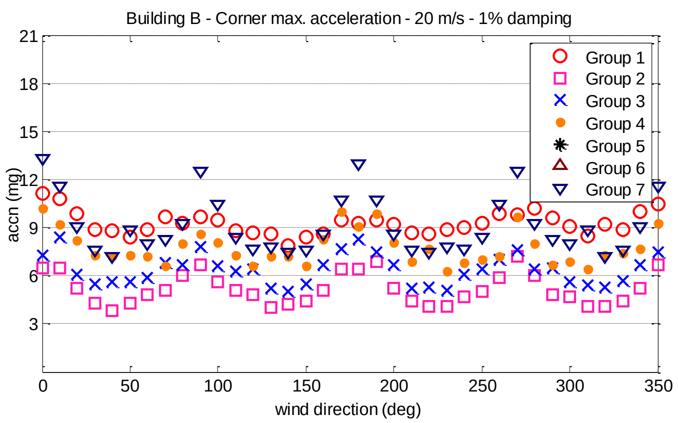

Fig. 9 Predicted corner accelerations for a mean wind speed of 20 m/s, 1% damping (Building B)

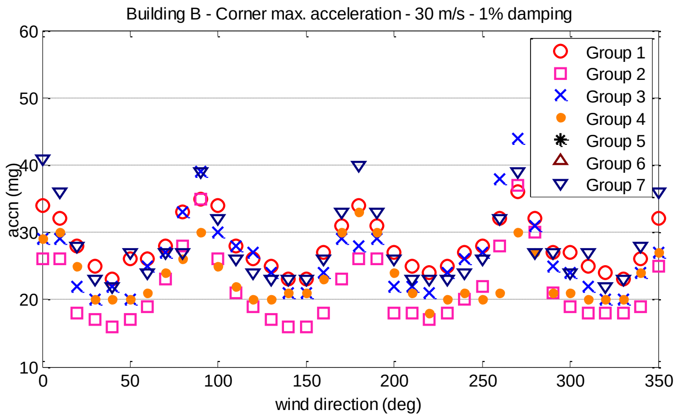

Fig. 10 Predicted corner accelerations for a mean wind speed of 30 m/s, 1% damping (Building B)

Fig. 10 shows similar results to those in Fig. 9, but for a mean wind speed at the top of the building of 30 m/s. This wind speed represents approximately a 5 to 20 year return period value for many locations in the world. The measured peak accelerations are approximately three times those in Fig. 9, corresponding to a variation with mean wind speed with an average exponent of about 2.7. The scatter between groups is generally lower than that in Fig. 9, probably related to the greater measurement accuracy in measuring spectra at the lower reduced frequencies associated with the higher wind speed, i.e., the bandwidth of the measurement system is less critical.

The simulation by one group had a longitudinal turbulence intensity significantly lower than the specified target value at the top of the building (see Appendix A, Fig. A2). This would have affected the fluctuating base moments and accelerations – probably by reducing the along-wind responses, and increasing the cross-wind responses.

3. Comparison of advanced building results

The ‘advanced’ building, denoted as Building A, is a modified version of a 60-story benchmark building with height of 240 metres, already in use for vibration control applications (Tse *et al*. 2007). This building is also of uniform rectangular cross-section with dimensions of 72 metres by 24 metres. The dynamic properties are summarized in Table 1 and Fig. 11. Only the first three of the original six modes have been specified for the HFBB benchmark tests. The main modification was the introduction of more lateral-torsional coupling for the second and third modes. Hence, the three modes are all coupled to provide more of a challenge for the HFBB processing techniques.

Table 1 Dynamic Properties of Building A

Mode	Coupling of Modes	Frequency (Hz)	Damping (% of critical)
1	predominantly sway-y & twist	0.231	1 and 2.5
2	predominantly sway-x & twist	0.429	1 and 2.5
3	twist, sway-x & sway-y	0.536	1 and 2.5

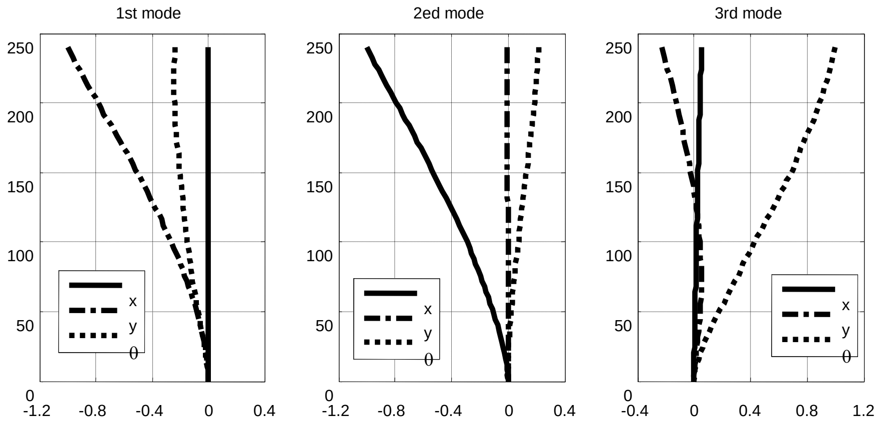

Fig. 11 Mode shapes for Building A

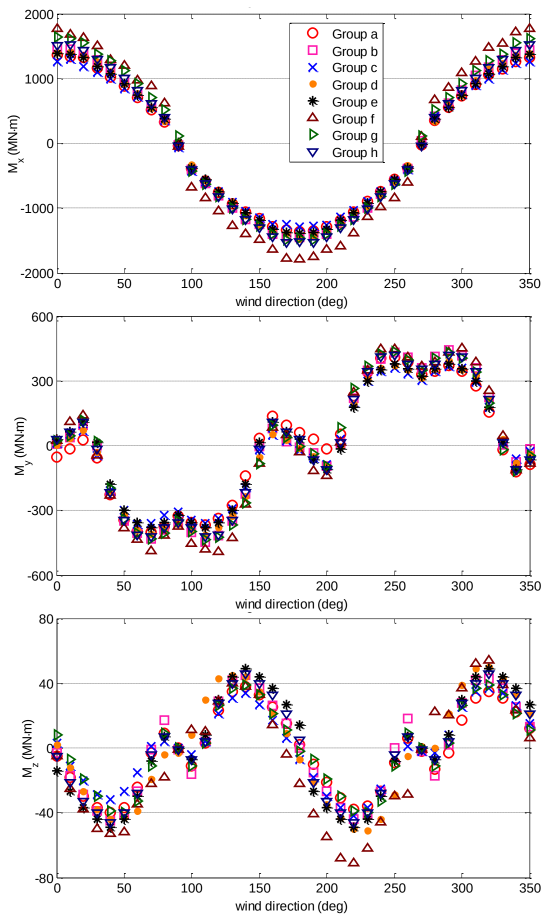

Fig. 12 Mean base moments ($\overline{U}_h$ = 30 m/s) for Building A

3.1 Base moment comparison – Building A

Eight groups submitted results for this building, which have been corrected to a sea level density of 1.20 kg/m^3 prior to the following comparisons. To avoid redundancy, only the results for a mean wind speed at the top of the building of 30 m/s are shown in Fig. 12.

Similar to the Building B, the mean sway moments show reasonably good agreement while the mean torsional moments show slightly more scatter. The coefficients of variation are approximately 20%.

The dynamic base moments were subsequently calculated by each group based on the supplied structural dynamic properties, including natural frequencies, mode shapes, mass distribution and story mass centres. The predicted *maximum* base moments about the x-axis for a wind speed of 30 m/s and critical damping ratio of 1.0%, are shown in Fig. 13. *Minimum* base moments about the y-axis are shown for the same wind speed and damping in Fig. 14. The maximum torsional moments about the z axis are shown in Fig. 15. Higher coefficients of variation of over 20-30% are evidently observed, in particular for the torsional moments, which are largely attributed to the different mode shape correction factors and modal combination methods used to account for the nonlinear mode shapes and lateral-torsional coupling, respectively.

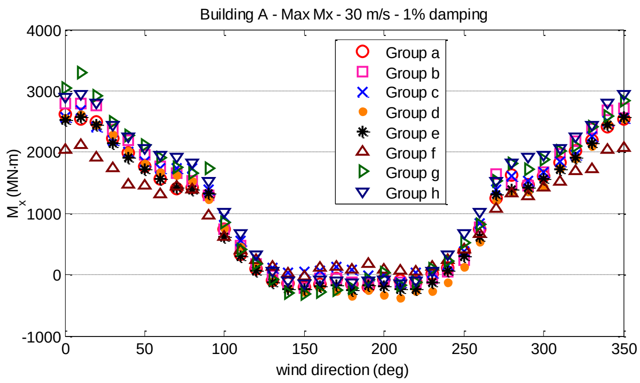

Fig. 13 Predicted maximum sway moments about the x-axis (Building A)

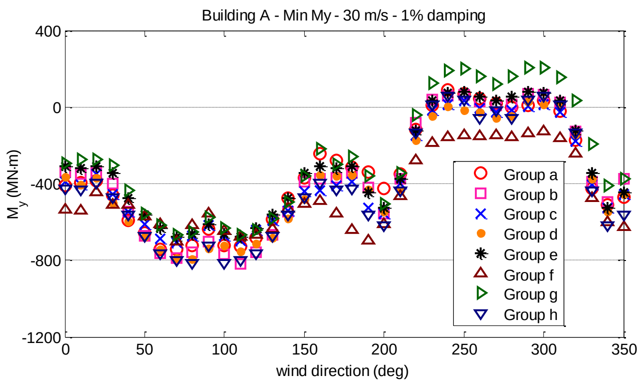

Fig. 14 Predicted minimum sway moments about the y-axis (Building A)

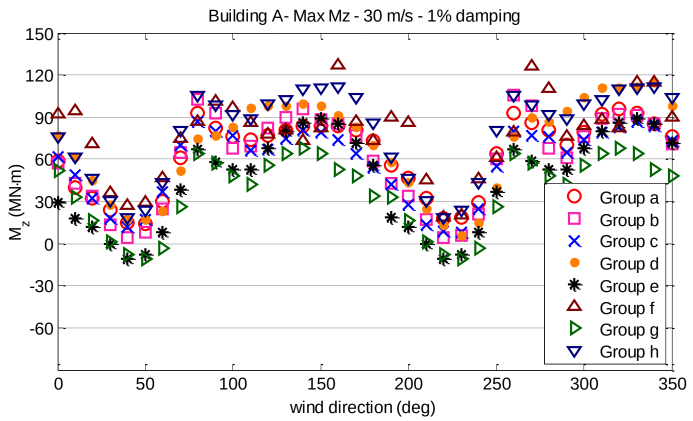

Fig. 15 Predicted maximum twist moments about the z-axis (Building A)

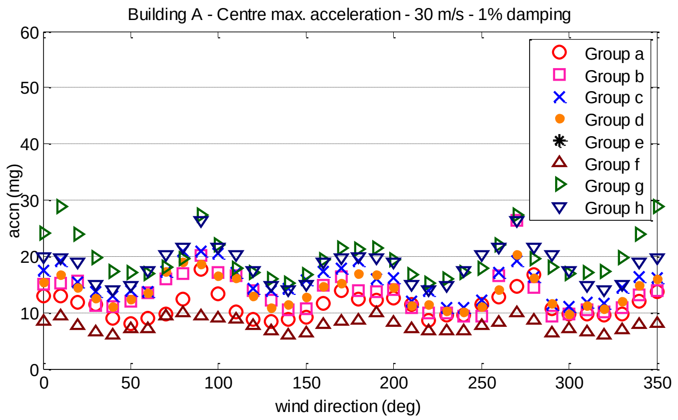

Fig. 16 Predicted centre accelerations for a mean wind speed of 30 m/s, 1% damping (Building A)

3.2 Comparison of accelerations – Building A

Seven out of eight participating groups provided resultant accelerations at the top of the building at the geometric centre, and at a corner of the roof. Figs. 16 and 17 show predicted maximum accelerations at the centre and corner, respectively, for a mean wind speed at the top of the building of 30 m/s and critical damping ratio of 1%. The predicted accelerations at the top of Building A are generally lower in magnitude than those for Building B, (compare Fig. 17 to Fig. 10). This is probably relates to the higher frequencies of Building A.

The predicted maximum accelerations are more scattered than for Building B, for both the centre, and corner, of the building; this can be attributed to the reasons stated in the preceding section, as well as the methods used for combining acceleration components. Specifically, five out of eight participating groups used the square-root-of-sum-of-square (SRSS) method without a reduction factor to compute the resultant accelerations (i.e., vector sum of two translational components at building geometric centre and two translational components plus one torsional component at building corner). The other groups used different methods with an equivalent reduction factor ranging from 0.8-0.9, which takes into account the contribution of dominant component over the others. If this reduction factor was applied along with the SRSS method, the coefficient of variation of estimated accelerations among groups would be reduced from 26-39% to 22%-36%. In addition, the scatter in the acceleration predictions can be attributed to the accurate measurement of spectra of generalized forces at high reduced frequencies, which could be considerably influenced by the model's fundamental frequency. Some groups simply used the measured force spectra for the subsequent analysis. Whist some groups have attempted to remove the model/balance resonance from the generalized force spectra, resulting in a relatively lower acceleration prediction.

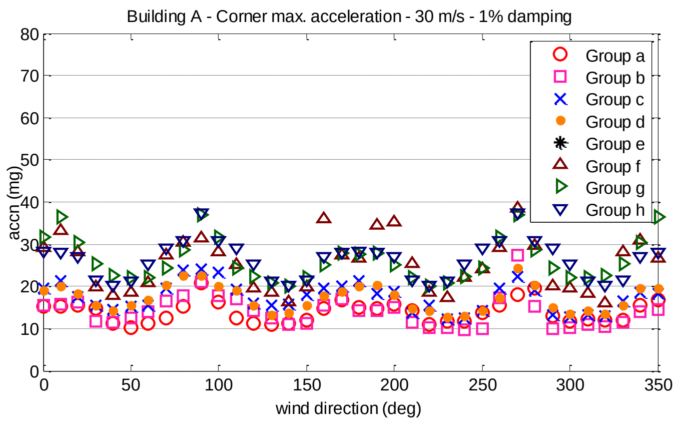

Fig. 17 Predicted corner accelerations for a mean wind speed of 30 m/s, 1% damping (Building A)

4. Conclusions

Some comparisons from the International HFBB study have been presented in this paper. The results shown represent a small proportion of the total amount of material presented, but illustrate the main trends in the comparisons.

The mean and peak base moments from the participating groups show quite good agreement with coefficients of variation about the averages of 8-20% for Building B and 20-30% for Building A. The peak corner accelerations from five groups show greater variation, especially for the lowest wind speed. The greater scatter in the acceleration predictions can be attributed to the dominance of the resonant components, which rely on accurate measurement of spectra of generalized forces at relatively high reduced frequencies requiring higher bandwidth in the instrumentation, a known difficulty with the HFBB technique. For buildings with nonlinear 3-dimensional mode shapes (i.e., lateral-torsional coupling), such as Building A in this study, the greater scatter in the predictions can be attributed to the usage of different mode shape correction factors, modal combination methods, and methods for combining acceleration components among the groups.

Acknowledgements

The authors acknowledge with gratitude all the participating groups in this study for their cooperation in providing data in a timely fashion, and for their willingness in having their measurement techniques put under scrutiny. The authors also thank one of the groups for providing images for Fig. 3. Finally the authors are grateful for the comments by the reviewers; these have resulted in changes that have improved the paper considerably.

References

Tschanz, T. and Davenport, A.G. (1983), "The base balance technique for determination of dynamic wind loads", *J. Wind Eng. Ind. Aerod.*, **13**(1-3), 429-439.

Boggs, D.W. and Peterka, J.A. (1989), "Aerodynamic model tests of tall buildings", *J. Eng. Mech. - ASCE,* **115**(3), 618-635.

Holmes, J.D., Tse, K.T., Ho, T.C. and Boggs, D. (2008), "Benchmark buildings for high-frequency base balance tests", *Proceedings of the 4th International Conference on Advances in Wind and Structures* (AWAS'08), Jeju, Korea, 29-31 May 2008.

Melbourne, W.H. (1980), "Comparisons of measurements on the CAARC Standard tall building model in simulated model wind flows", *J. Wind Eng. Ind. Aerod.*, **6**(1-2), 73-88.

Tse, K.T., Kwok, K.C.S., Hitchcock, P.A., Samali, B. and Huang, M.F. (2007), "Vibration control of a wind-excited benchmark tall building with complex lateral-torsional modes of vibration", *Adv. Struct. Eng.*, **10**(3), 283-304.

Appendix A

The boundary-layer flow properties specified were similar for both buildings. They are summarized below:

Design mean wind speed at top of building (both cases): 20, 30 and 40 m/s (assumed uniform with wind direction)

Urban terrain. Mean velocity profile. Power law exponent: 0.25
(approximate roughness length z_0 : 0.2 mm)

Longitudinal turbulence intensity at rooftop of building B: 0.143
Longitudinal turbulence intensity at rooftop of building A: 0.131

Lateral and vertical intensities: not specified.

Integral turbulence length scale at rooftop height of building B: 175 m
Integral turbulence length scale at rooftop height of building A: 190 m

Mean velocity profiles and longitudinal turbulence intensity profiles supplied by four groups are shown plotted in Figs. A.1 and A.2 respectively.

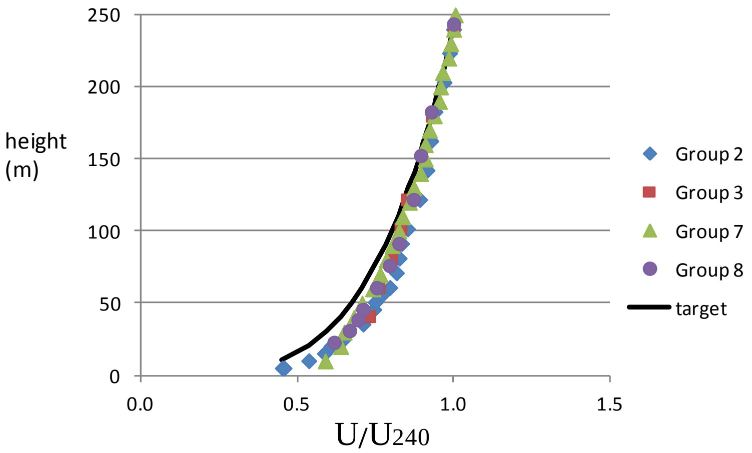

Fig. A.1 Mean velocity profiles compared with target profile

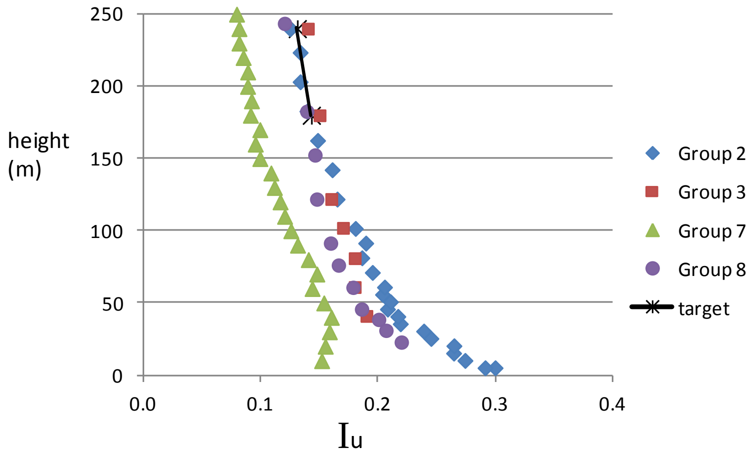

Fig. A.2 Turbulence intensity profiles compared with target values